

Static and Switching Characteristics of 6500 V Silicon Carbide Anode Switched Thyristor Modules

Siddarth Sundaresan, Aye-Mya Soe, Ranbir Singh

GeneSiC Semiconductor Inc.
Dulles, VA 20152, USA

Abstract— Silicon Carbide Anode Switched Thyristors (ASTs) overcome major limitations of conventional Si and SiC IGBT and GTO Thyristor solutions by providing robust, MOS-controlled, turn-off at high currents, current saturation in the output characteristics through series current controlled device turn-off. In this work, detailed static and switching characteristics of 6.5 kV-class SiC ASTs are reported, which include a low on-state voltage drop of 4 V at 100 A/cm², slight positive temperature co-efficient of Von, current saturation at > 100 A Cathode currents and fast turn-on and turn-off times of < 2 μ s while switching 3600 V and 14.5 A. The transient voltages seen by the Si MOSFETs during AST switching are examined to determine safe operating area limits for this circuit configuration.

I. INTRODUCTION

The SiC Anode Switched Thyristor (AST) is being developed by GeneSiC for high efficiency power conversion at > 13 kV, > 50 A and > 10 kHz ratings for applications like Flexible AC transmission systems (FACTS), Fault-Current Limiters, AC-DC converters, and Static VAR Compensators. Presently, utility-connected power electronics hardware use Insulated Gate Bipolar Transistors (IGBTs) and various flavors of Thyristor devices [1]. IGBTs offer easy MOS-control, but are not available at high enough ratings. Besides, they are difficult to implement in Silicon Carbide. On the other hand, both Si and SiC Thyristors are difficult to turn-off without the aid of di/dt and dV/dt snubbers. In contrast to conventional SiC Thyristors, the SiC AST, which is similar to a SiC Emitter Turn-Off (ETO) Thyristor [2], offers MOS gate control, current saturation capability and fast switching speeds. The AST eliminates the need for turn-on and turn-off snubber circuitry, which is essential for convenient operation of conventional Thyristors. The detailed on-state, blocking voltage and switching characteristics of 6.5 kV-rated SiC ASTs are presented in this paper.

II. DESIGN AND FABRICATION OF THE SiC AST

A schematic of the AST circuit is shown in Figure 1 and a photograph of the fabricated AST module is shown as an inset in Figure 1. In an AST, the turn-on and turn-off of a high-voltage SiC GTO Thyristor is accomplished by high-current commercially available Si MOSFETs and gate drivers. The AST is turned-on from its blocking state by

providing a negative Gate current trigger pulse, which latches-on the SiC GTO Thyristor and turns-on a p-MOSFET connected in series with the Thyristor Anode. To turn-off the AST, the Gate pulse is withdrawn, which turns off the p-MOSFET and subsequently turns on a diode-connected n-MOSFET connected to the Thyristor Gate electrode, when the threshold voltage of the n-MOSFET is exceeded. The turning-off of the p-MOSFET and turning-on of the n-MOSFET commutates the entire Anode current to the Gate path of the AST. This results in a collapse of the “Thyristor Action”, and the AST turns-off like an open base npn transistor with a rapid, unity-gain turn-off.

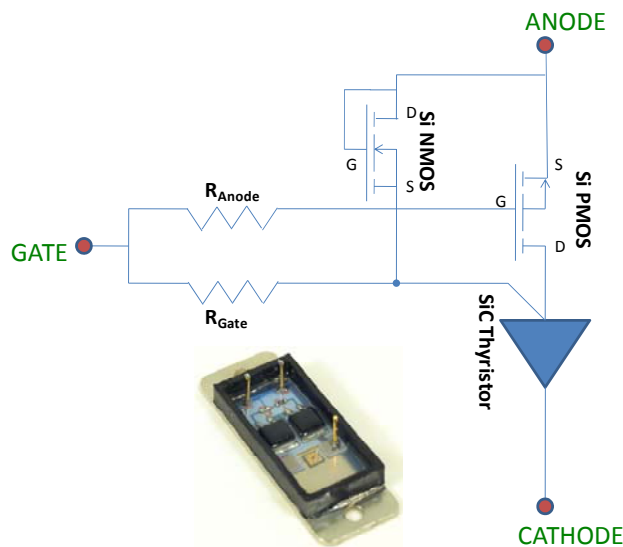


Figure 1. Simplified Circuit-level schematic of the SiC AST Module (Inset) Photograph of a fully assembled AST module populated with the SiC GTO Thyristor, Si MOSFETs and the series resistors.

The key design parameters for the SiC AST include the development of high turn-off current gain SiC GTO Thyristors, selection of appropriate Si N-Channel and P-Channel MOSFETs with the appropriate voltage/current ratings and suitable threshold voltages, such that they turn-on and turn-off at appropriate times during the AST switching and do not introduce excessive series resistance during on-state operation. In the present work, a 4.1 mm x 4.1 mm SiC

GTO Thyristor (see ref.[3] for design and fabrication details) with active area of 7.3 mm^2 , 75 V/90 A Si n-MOSFETs with a Gate threshold voltage of $\approx +4.5 \text{ V}$ and a 85 V/96 A Si p-MOSFETs were used in the AST circuit. A key feature of this work was the co-packaging of the Si MOSFETs and the SiC GTO Thyristor on the same ceramic baseplate with the appropriate voltage isolation necessary for high blocking voltages and high-temperature capability up to $125 \text{ }^\circ\text{C}$, as shown in Figure 1.

III. ON-STATE CHARACTERISTICS OF THE SiC AST

At 100 A/cm^2 (with respect to the active area of the SiC Thyristor) and $25 \text{ }^\circ\text{C}$, the integrated AST shows a slightly higher $V_{on} = 4.0 \text{ V}$ as compared to the SiC GTO Thyristor, which has a low $V_{on} = 3.8 \text{ V}$, as shown in Figure 2(a). This is due to the additional on-resistance of the series p-MOSFET. From the $25 \text{ }^\circ\text{C}$ output characteristics at 100 A/cm^2 , a higher differential on-resistance of $5.6 \text{ m}\Omega\text{-cm}^2$ is extracted for the AST in comparison with $3.9 \text{ m}\Omega\text{-cm}^2$ for the SiC GTO Thyristor. The SiC GTO Thyristor shows a negative temperature co-efficient of V_{on} in Figure 1(a), due to an increase in recombination carrier lifetime and a reduction of the p-n junction knee with temperature. However, the SiC AST shows a slight positive temperature co-efficient of differential on-resistance, because the increase in the on-resistance of the series-connected p-MOSFET opposes the reduction of the knee-voltage and carrier lifetime increase in the base layer of the SiC GTO Thyristor. The current saturation capability of the SiC AST in contrast to the SiC GTO Thyristor is shown through high-current static I-V characteristics in Figure 1(b). At Cathode currents $> 90 \text{ A}$ (1300 A/cm^2 for the SiC GTO Thyristor), the presence of the Si MOSFET allows for a self-saturation of the AST I-V characteristic, which is a desirable feature for over-current fault protection. However, it is worth pointing out that since the current flow in the AST is controlled through the 85 V-rated p-channel Si MOSFET, current saturation of the AST output characteristics will not be observed at higher voltages in excess of the breakdown voltage rating of the Si MOSFET.

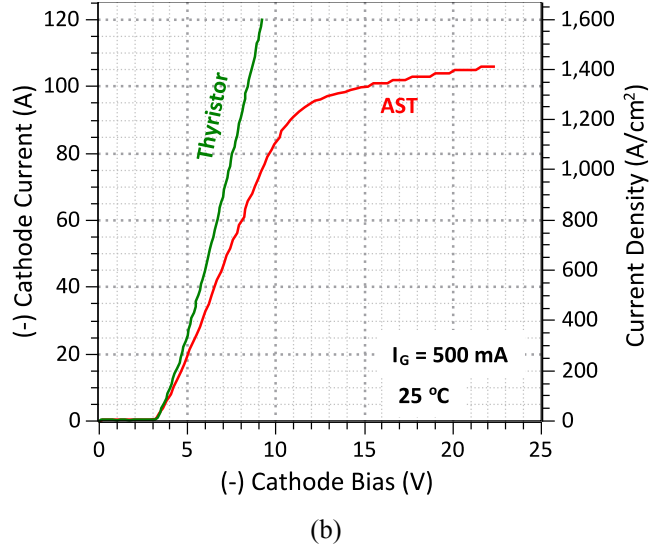
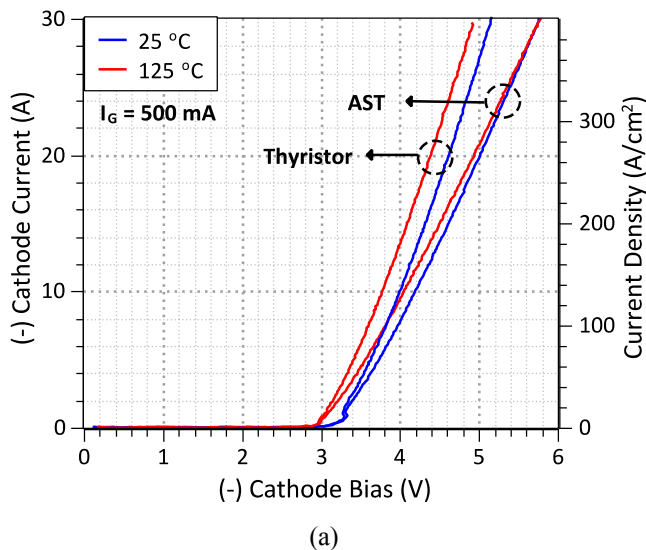


Figure 2. (a) Output characteristics of the SiC AST module and the constituent SiC GTO Thyristor and (b) Current Saturation displayed by the SiC AST at high Cathode current densities.

IV. BLOCKING VOLTAGE CHARACTERISTICS

The open-Gate blocking voltage of the SiC AST was measured to be in excess of 3 kV at $125 \text{ }^\circ\text{C}$, limited by the currently used packaging techniques. The blocking characteristics of a $5.25 \text{ mm} \times 5.25 \text{ mm}$, 6.5 kV SiC GTO Thyristor is compared at $25 \text{ }^\circ\text{C}$ and at $150 \text{ }^\circ\text{C}$ with a commercial 4 kV Silicon Thyristor in Figure 3. The Si Thyristor displays extremely high leakage currents at $125 \text{ }^\circ\text{C}$, due to its large device size and low (1.1 eV) bandgap for Si, as compared to 3.2 eV for 4H-SiC. Only a modest increase in leakage current is measured on the SiC GTO Thyristor at $150 \text{ }^\circ\text{C}$, validating the high-temperature operation capability of high-voltage SiC GTO Thyristors.

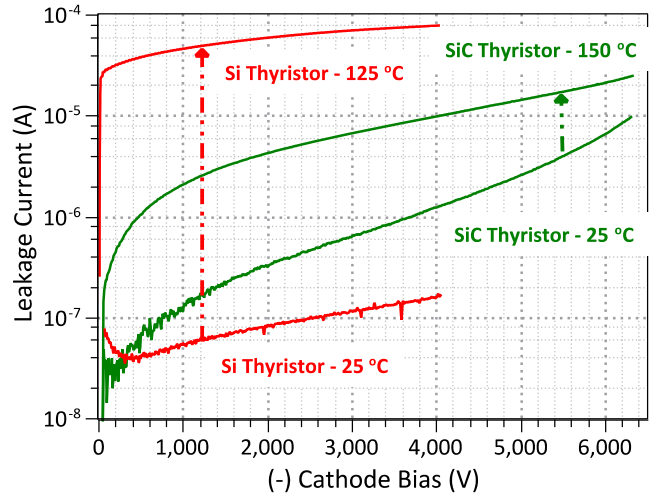


Figure 3. Comparison of blocking characteristics of a $6.5 \text{ kV}/5.25 \text{ mm} \times 5.25 \text{ mm}$ SiC GTO Thyristor with an off-the-shelf 4 kV Si GTO Thyristor at different temperatures.

V. SWITCHING CHARACTERISTICS OF THE SiC AST

A. Mixed Resistive-Inductive Load Test Circuit

Switching characteristics of the SiC ASTs up to 1380 V and 20 A under a resistive load were previously demonstrated in [4]. In the present work, the switching characteristics of the SiC ASTs were obtained under a mixed resistive-inductive load configuration as shown in Figure 4. A 10 μF capacitor is charged to the desired voltage using a power supply, and an appropriately chosen load inductor is used to achieve a certain load current ramp rate. A 10 kV/10 A SiC JBS rectifier fabricated at GeneSiC is used as the free-wheeling diode. Differential voltage probes are used to measure the voltage across the p-MOSFET M2, and the voltage across the Cathode and Anode of the AST. A third passive voltage probe measures the Gate voltage, while a Pearson current transformer is used to monitor the Cathode current. The Gate terminal of the AST was driven between -11 V and 0 V. R_{Anode} and R_{Gate} values of 10 Ω and 100 Ω , respectively, were used for all the switching experiments.

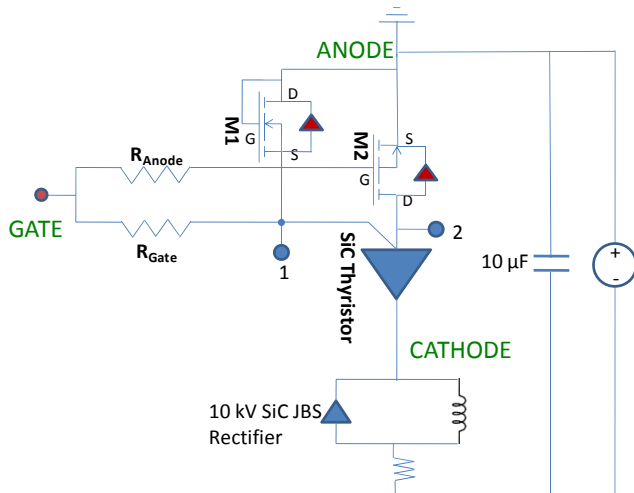


Figure 4. Schematic of the mixed resistive-inductive load circuit used for switching characterization of the SiC ASTs. Voltage probing points are provided at the AST Cathode, Gate terminals and at nodes 1 and 2 as shown in the schematic. A Pearson current transformer measures the Cathode current of the AST. The internal free-wheeling diodes associated with the Si MOSFETs are also shown for better understanding of circuit operation.

B. Voltage and Current Transients during typical AST Switching

To illustrate the SiC AST operation, voltage and current waveforms from a 1500 V/5.5 A switching measurement are shown in Figure 5. Initially, the AST is the blocking state, with most of the Cathode bias supported across its Anode and Cathode terminals. The voltage, V_{G1} is measured at node 1 in Figure 5. For turning ON the AST, a (constant) Gate pulse of -11 V is supplied via an optically isolated Gate driver, which turns on the p-MOSFET, and also establishes a Gate current of ≈ 100 mA for turning ON the SiC GTO Thyristor. Notice that V_{G1} increases with V_G but is then clamped at the approximately the Anode-Gate voltage (3-3.5 V) across the Thyristor, once the p-MOSFET turns-ON. V_{G1}

needs to be maintained below the threshold voltage of the NMOSFET, to keep it turned off during the AST conduction period. For turning off the AST, the Gate bias is increased from -11 V to 0 V, which turns-off the PMOSFET. This causes the diode-connected NMOSFET to turn-ON and it draws the entire Cathode current, due to the inductive load characteristic. The Cathode voltages then starts rising toward the capacitor voltage, as the depletion regions are established within the SiC GTO Thyristor. Finally, the Cathode current turns-off, and the AST enters the blocking (OFF) state.

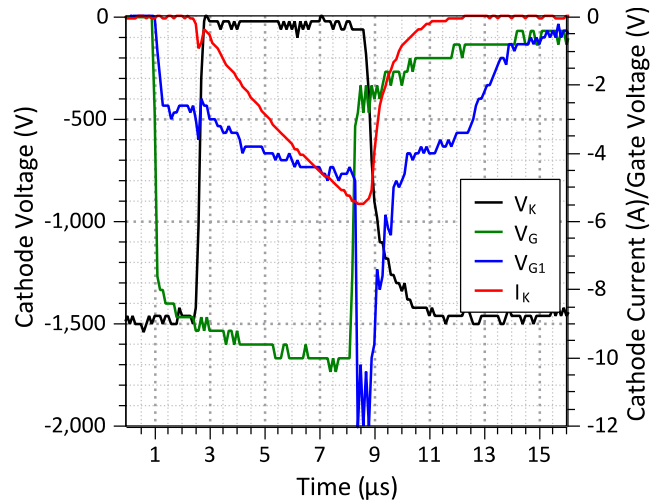


Figure 5. Typical switching waveforms measured across various terminals of the SiC AST Module during a power switching demonstration. The SiC AST switches 1500 V and 5.5 A in this example, under a mixed resistive-inductive load configuration. V_{G1} is the voltage measured at node 1 (refer to Figure 4).

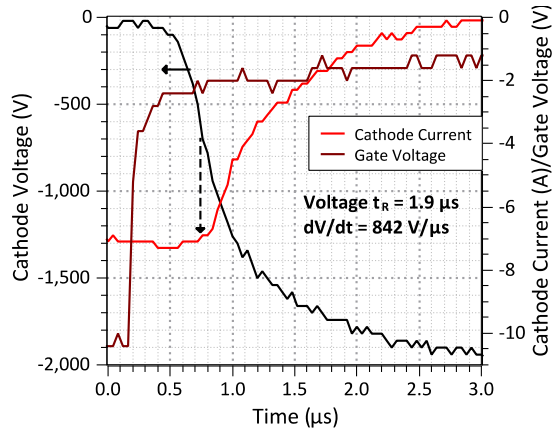
Unique Advantages of the SiC AST Configuration:

During AST turn-OFF, the entire Thyristor current is commutated automatically through the Gate electrode of the SiC GTO Thyristor (unity-gain turn-off) and the n-MOSFET to ground. The AST turns OFF like an open-base NPN transistor, and no self-sustaining current latchup (Thyristor) action remains. Another useful feature of the AST evident from Figure 5 is that the Gate terminal of the AST is isolated from the high Cathode currents which are diverted via the Gate electrode of the Thyristor and the series n-MOSFET to ground.

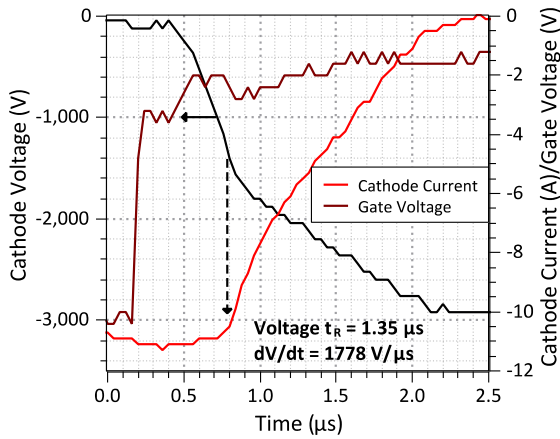
C. High-Voltage AST Switching Measurements

The turn-off for mixed resistive-inductive load switching waveforms with progressively increasing voltages/current measurements at 2000 V/7 A, 3000 V/11.5 A and 3600 V/14.5 A were taken on ASTs. The resulting AST Cathode Voltage, Cathode Current, and Gate voltage waveforms are shown in Figure 6. Delay times of 0.5 μs , and Cathode Voltage Rise Times of the order of 1.35-1.9 μs are observed from the switching measurements. As the Cathode Bias is increased from 2000 V to 3600 V, the Cathode Voltage/Current waveforms appear to distinctly show three different regions with different dI/dt and dV/dt , indicative of different rates of carrier recombination in the Thyristor upper and lower base regions and in the punch-through buffer

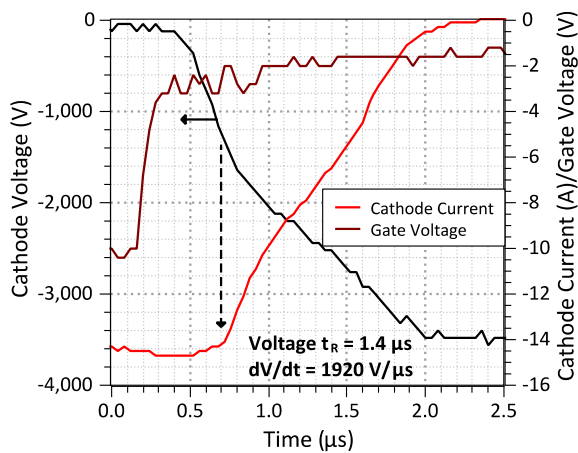
layers. Cathode Voltage turn-off dV/dt of $842\text{ V}/\mu\text{s}$ to $1920\text{ V}/\mu\text{s}$ are observed for the different switching waveforms. The Cathode Current dI/dt is maintained below $50\text{ A}/\mu\text{s}$ by the inductive load.



(a)



(b)

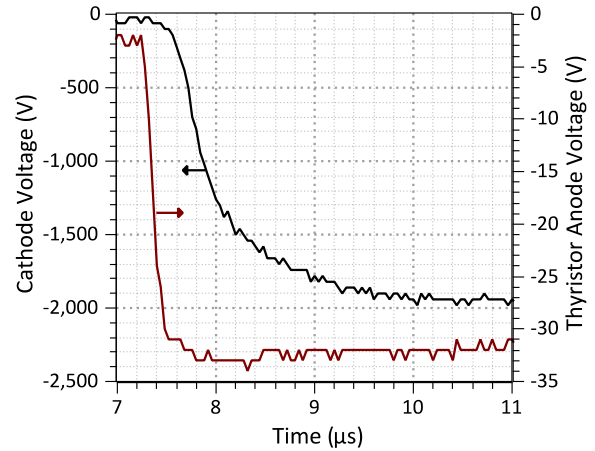


(c)

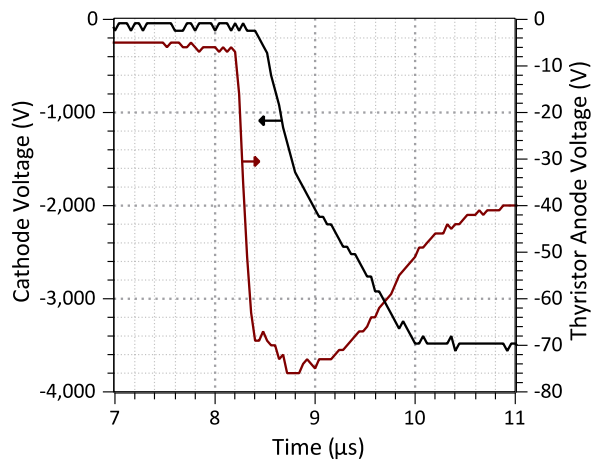
Figure 6. Cathode Voltage/Current and Gate Voltage switching waveforms obtained during turn-off characterization of the 6.5 kV-Class SiC AST at (a) $2000\text{ V}/7\text{ A}$, (b) $3000\text{ V}/11.5\text{ A}$ and (c) $3600\text{ V}/14.5\text{ A}$.

VI. HIGH TRANSIENT VOLTAGES EXPERIENCED BY SILICON MOSFETS IN THE AST CIRCUIT

While it is true that during steady-state blocking mode conditions, most of the high DC link voltages for the 6.5 kV-class AST presented in this paper will be supported by the SiC Thyristor, the Si p-MOSFET in series with the SiC Thyristor can experience high peak voltages during the turn-off transient, since it turns-off faster than the SiC Thyristor. During the AST switching measurements, an additional voltage probe was inserted to monitor the voltage at the SiC Thyristor Anode (or Node 2 in Figure 4), which corresponds to the voltage across the Si p-MOSFET. From the switching transients shown in Figure 7, it can be clearly seen that the voltage experienced by the p-MOSFET is higher, when turn-off measurements are conducted at higher Cathode biases. At a Cathode bias of 3600 V , the p-MOSFET experiences a transient voltage as high as 75 V , which is slightly lower than its breakdown rating of 85 V . It is however possible to reduce these high transient voltages across the p-MOSFET by increasing the Gate resistor used for driving the p-MOSFET.



(a)



(b)

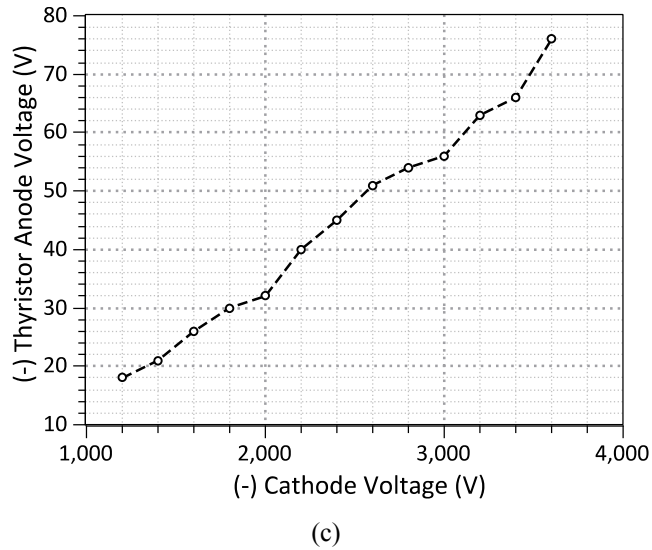


Figure 7. Cathode Voltage and Thyristor Anode (or Node 2) Voltage switching waveforms obtained during turn-off characterization of the 6.5 kV-Class SiC AST at (a) 2000 V/7 A, and (b) 3600 V/14.5 A. (c) A plot of the peak voltage experienced at the Thyristor Anode as a function of the Cathode Bias used for the AST switching measurement.

VII. CONCLUSIONS AND FUTURE WORK

The static and switching characteristics of 6.5 kV SiC ASTs up to 3600 V and 14.5 A were presented in this paper. The unique advantages of the SiC AST circuit configuration

over a standard GTO Thyristor for high-current and high-voltage turn-off were elucidated by detailed experimental characterization. A thorough analysis of the voltage and current transients experienced by each component in the AST circuit was performed and potential issues with the AST configuration were discussed. High-temperature measurements of the SiC ASTs are currently in progress to examine the temperature dependence on the current and voltage transients of the ASTs. Results from these measurements and a detailed reliability investigation of the electrical characteristics of the SiC ASTs including RBSOA will be discussed in a future article.

VIII. REFERENCES

- [1] U. Schwarzer, R.W. De Doncker, "Characterization of 6.5 kV IGBT Modules for hard- and soft- switching operation in medium voltage applications", Proceedings of Applied Power Electronics Conference and Exposition (APEC), pp. 329-335 (2005).
- [2] J. Wang A.Q. Huang, "Design and Characterization of High-Voltage Silicon Carbide Emitter Turn-Off Thyristor", IEEE Trans. Power Electronics, 24(5), pp.1189-1197 (2009).
- [3] S.G. Sundaresan, H. Issa, D. Veerreddy, R. Singh, "Large Area >8 kV SiC GTO Thyristors with Innovative Anode-Gate designs", Mater. Sci. Forum 645-648, pp.1021-1024 (2010).
- [4] S.G. Sundaresan, E. Lieser, R. Singh, "Integrated SiC Anode Switched Thyristor Modules for Smart-Grid Applications", Mater. Sci. Forum 717-720, pp. 1159-1162 (2012).